Cardiovascular Diabetology

RESEARCH

Open Access

Proteomics-derived organ-specific aging clusters predict macrovascular and microvascular complications in diabetes

Sheng Yuan[1,2†], Zhangyu Lin[1,2†], Yanjun Song[1,2†], Ketai Shi[3], Jingjing Guan[4], Zhiyong Zhao[2,5*] and Kefei Dou[1,2,5,6*]

Abstract

Background Aging is intrinsically linked to diabetes pathogenesis, yet evidence gaps persist regarding organ-specific aging and risks of long-term diabetes complications. This study aims to estimate the association between plasma proteomics-based organ-specific aging and risks of long-term diabetes complications.

Methods This cohort study quantified biological age gaps (residuals from linear regression of predicted versus chronological age) across 11 organ systems in 1979 baseline diabetes patients based on plasma proteomic profiling (Olink Explore 3072) of 2916 proteins and three validated different aging models. Extreme aging was defined as > 1.5 standard deviation from organ-specific mean age gaps. Multivariable Cox models assessed incident complication risks in 1707 complication-free patients.

Results During a median follow-up time of 12.71 years, 356 incident all-cause deaths (20.86%), 348 incident cardiovascular disease (CVD) (20.39%), 227 incident diabetic retinopathy (DR) (13.30%), 88 incident peripheral artery disease (PAD) (5.16%), and 280 incident chronic kidney disease (CKD) (16.40%) occurred. Extreme cardiac aging showed strongest CVD risk association (adjusted HR: 2.92, 95% CI: 2.13, 3.99; $P < 0.001$), with significant brain (adjusted HR: 1.43, 95% CI: 1.06, 1.92; $P = 0.019$), arterial (adjusted HR: 1.59, 95% CI: 1.06, 2.39; $P = 0.024$), and pancreatic (adjusted HR: 1.35, 95% CI: 1.04, 1.77; $P = 0.027$) aging associations. Each complication demonstrated distinct organ-aging signatures. The association remains robust and consistent across three distinct aging models. Patients with baseline extreme aging in more than 3 organs faced significantly higher risks of incident diabetes complications compared to those with no or only one to three extremely aged organs. Additive interaction analysis revealed synergistic effects of organ aging on complications risk in diabetes. For example, concurrent heart and muscle aging substantially elevated CVD risk with a relative excess risk due to interaction (RERI) of 3.49 (95% CI: 0.74, 8.16) and an attributable proportion (AP) of 0.58 (95% CI: 0.14, 0.74).

†Sheng Yuan, Zhangyu Lin, and Yanjun Song have contributed equally to this work.

*Correspondence:
Zhiyong Zhao
pumc_zhaozy@126.com
Kefei Dou
drdoukefei@126.com

Full list of author information is available at the end of the article

Conclusions Proteomics-based organ aging assessment identifies significant complication-specific vulnerability patterns and substantially elevated risks with multiorgan involvement, supporting comprehensive aging evaluation for diabetes risk stratification. These findings require further validation in larger and more diverse populations and warrant more precise characterization of organ-specificity to enhance their robustness and generalizability.

Keywords Diabetes, Complications, Proteomics, Aging

Research insights

What is currently known about this topic?

- Cellular senescence in multiple tissues, including pancreatic β-cells, has been established as a key contributor to diabetes pathogenesis.
- Recent advances in proteomics have enabled plasma proteomics-based assessment of organ-specific aging.
- Diabetes complications involve multiple organs, severely impairing prognosis and quality of life.

What is the key research question?

- Can proteomics-based organ-specific aging predict the risk of major diabetes complications?

What is new?

- Organ aging exhibits significant associations with multiple diabetes complications.
- Organ aging manifests cumulative effects: complication risks escalate with the number of aging organs.
- Concurrent aging of two organs synergistically accelerates complication development.

How might this study influence clinical practice?

- Comprehensive proteomic profiling and multiorgan aging assessment in diabetes patients may enable holistic complication risk stratification.

Background

The rising global prevalence of diabetes has increased morbidity from major complications including cardiovascular disease (CVD), diabetic retinopathy (DR), peripheral artery disease (PAD), and chronic kidney disease (CKD) [1, 2]. Without early detection or intervention, these conditions may progress to severe outcomes such as heart failure, blindness, diabetic foot complications, and end-stage renal disease, significantly reducing life expectancy and quality of life [3, 4]. Early risk prediction before complication onset is therefore imperative for identifying candidates who would benefit most from preventive interventions [5].

Rising diabetes prevalence and population aging are expected to increase complication rates substantially [6, 7]. Pancreatic β-cell senescence represents a key pathogenic mechanism in diabetes [8, 9]. While chronological aging progresses uniformly, biological age, which reflects true physiological state, diverges significantly between individuals of identical chronological age [10, 11]. Consequently, research focus has shifted toward biological age due to accumulating evidence of its stronger correlation with diabetes [12].

Plasma proteomics represents a highly promising prognostic approach for metabolic disorders, capturing dynamic interactions between genetic susceptibility and modifiable factors such as environmental exposures, lifestyle patterns, pharmacological treatments, and concurrent disease progression [13, 14]. Building on this foundation, recent large-scale proteomic analyses of over 44,000 individuals have established validated models quantifying biological aging in eleven major organs using plasma protein signatures, with these organ age metrics demonstrating significant associations with incident diseases and mortality in validation cohorts [15]. However, the predictive value of multi-organ aging profiles specifically for diabetes-related complications remains uncharacterized. This investigation leverages the UK Biobank cohort to estimate organ-specific aging in diabetes individuals and systematically evaluates their relationships with CVD, DR, PAD, CKD, and all-cause mortality.

Methods

Participants and proteomics

This study utilized data from the UK Biobank prospective cohort, comprising over 500,000 participants recruited from 22 assessment centers with ethical approval from the North West Multicenter Research Ethics Committee (Reference #11/NW/0382). All analyzed participants provided informed consent under UK Biobank application #97155. From 53,018 individuals with available plasma proteomics data, we excluded participants with > 1000 missing protein values (n = 8182), missing covariate data (n = 4889), or lacking follow-up information/withdrawn consent (n = 105), resulting in 1979 baseline diabetes patients for analysis. Proteomic quantification was performed through the UK Biobank Pharma Proteomics Project using the Olink Explore 3072 platform, which measured 2923 unique proteins via antibody-based proximity extension assay. After excluding proteins with > 10%

missing values, 2916 proteins were retained for analysis. The baseline cohort demonstrated high representativeness of the broader UK Biobank population, with full methodological details on participant composition and proteomic processing previously documented [16].

Definition and calculation of organ age

Organ-specific plasma proteins were selected according to prior methodology by identifying human genes exhibiting ≥ fourfold enrichment in expression within single organs relative to all other organs, utilizing bulk RNA sequencing data from the Gene Tissue Expression Atlas (GTEx) [17]. Organ-specific aging models were originally developed using LASSO regression to predict chronological age, with comprehensive methodological details published previously [15]. For full transparency, we report the key parameters and performance metrics of the models below:

1) *Training and test sets*: The models were trained on samples from 11 UKB collection centers (n = 23,140) and tested on samples from the remaining 11 centers (n = 21,358). Quality control included excluding samples with > 1,000 missing protein values (n = 8182) and proteins with > 10% missing values (n = 7), resulting in a final dataset of 44,498 samples with 2916 proteins.
2) *Model training*: LASSO regression was implemented with fivefold cross-validation to select the optimal λ (retaining 95% of peak prediction performance). Sparse models were generated using scikit-learn's LASSO function, with organ-enriched proteins as features for each organ-specific model.
3) *Performance metrics*: The organ-specific models exhibited stable performance across training and test sets. For instance, the brain aging model exhibited R^2 values of 0.505 in the training set (correlation coefficient r = 0.7106) and 0.504 in the test set (r = 0.7103), with corresponding mean absolute error (MAE) values of 4.61 years (training set) and 4.72 years (test set). The models were also validated in the Stanford ADRC/SAMS cohort to confirm robustness.
4) *Calculation of organ age gap and z-score*: For each model, we calculated the biological age discrepancy (age gap) as the residual term from linear regression of predicted age against actual chronological age. Predicted age was computed using the formula:

$$\text{Predicted Organ Age} = \text{Intercept} + \sum_{i=1}^{n} \beta_i \times \text{ z - scored Protein}_i$$

where n is the number of organ-enriched proteins for the target organ, β_i is the LASSO coefficient for protein i, and "z-scored Protein" is the plasma protein level normalized to the training set mean and standard deviation. Full coefficients (β_i) and intercepts for all 11 organ-specific models are provided in Supplementary Table S1.

To standardize these discrepancies across models accounting for variations in predictive accuracy, we converted age gaps into z-scores within each organ-specific aging framework. Participants demonstrating z-scored age gaps exceeding 1.5 standard deviations in any organ model were categorized as extreme agers.

Among the 2916 plasma proteins, 222 proteins (7.6%) were used as organ-enriched proteins. Each protein was exclusively assigned to one organ-specific clock (due to strict organ-enrichment criteria), ensuring no cross-contamination between organ models. The distribution of these proteins across organs is as follows: brain (30), artery (9), liver (51), immune system (79), intestine (13), lung (5), heart (2), pancreas (16), muscle (8), adipose (5), kidney (4).

To verify the stability of different proteomics-based organ aging assessment methods, we incorporated two additional models derived from Goeminne et al. [18] Briefly, Goeminne et al. analyzed plasma proteomics data from UK Biobank participants. Organ-specific proteins were defined as those with Genotype-Tissue Expression (GTEx) levels at least four times higher in one organ than in all other organs. The chronological aging model was trained with elastic net regression to predict chronological age, validated via fivefold cross-validation (correlation coefficient r = 0.94, MAE = 2.10 years in the test set). The mortality-based model used Cox proportional hazards elastic net regression to predict time-to-death, with similar cross-validation (r = 0.67, MAE = 0.55 in the test set) and demonstrated superior performance compared to established aging biomarkers like GrimAge. We obtained the full model coefficients from the supplementary materials of Goeminne et al. (also listed in supplementary Tables S2 and S3) and calculated organ-specific biological ages or predicted relative log(mortality hazard) for our cohort by applying these coefficients to the corresponding plasma protein levels available in the UK Biobank. The organ age gap was defined as the residual from regressing predicted biological age on chronological age, consistent with the original LASSO model. Both the age gap and log(mortality hazard) were z-scored within each aging model to normalize for differences in prediction accuracy.

Definition of diabetes and complications

Diabetes diagnosis required either hospital identification through ICD codes (ICD-10: E10-E14; ICD-9: 250) or baseline HbA1c ≥ 6.5%. We defined clinical outcomes

using hospital records: cardiovascular disease (CVD) encompassed heart failure (ICD-10: I50; ICD-9: 428), myocardial infarction (ICD-10: I21-I23; ICD-9: 410, 412), and stroke (ICD-10: I60-I66; ICD-9: 430, 431, 433, 434, 436); diabetic retinopathy (DR) used ICD-10: H36.0/ICD-9: 3620; peripheral artery disease (PAD) included ICD-10: I73.1, I73.8-I73.9, I74.2-I74.5/ICD-9: 443–444; chronic kidney disease (CKD) comprised ICD-10: I12.0, I13.1, I13.2, N18.0, N18.3-N18.5, N18.8, N18.9/ICD-9: 585. Mortality data originated from the UK National Health Service Central Register, National Records of Scotland (censored 30 November 2022), and NHS England (censored 30 November 2022).

Statistics

Protein concentrations underwent standardization using the mean and standard deviation from the primary deviation cohort as previously reported [15]. Continuous variables are presented as median with interquartile range (IQR) for non-normally distributed data or mean with standard deviation (SD) for normally distributed data, while categorical variables appear as frequencies with percentages. To comprehensively assess the predictive performance of organ-specific aging models, we calculated both Pearson correlation coefficients (r) between predicted organ-specific age and chronological age, and MAEs. MAE was defined as the average of the absolute differences between predicted and chronological age. Phi coefficients (ϕ) were employed to evaluate associations between binary variables. Differences in organ age gaps between participants with and without baseline diabetes complications were analyzed using age- and sex-adjusted linear regression. Multivariable Cox proportional hazards models quantified associations between organ age gaps (continuous) or extreme organ aging status (binary) and incident diabetes complications (CVD, DR, PAD, CKD) plus all-cause mortality, with Benjamini–Hochberg false discovery rate correction applied to *P* values. Adjusted covariates comprised age, sex, ethnicity, Townsend deprivation index (TDI), current smoking status, antihypertensive/antidiabetic medication use, systolic blood pressure (SBP), body mass index (BMI), total cholesterol, and glucose levels. To assess potential overfitting of the Cox regression models, Bootstrap validation with 1000 resamplings was performed, and the optimism value was calculated for each study endpoint as the core metric to quantify the degree of overfitting, which reflects the gap between the model's apparent performance in the training set and its actual generalization performance in unseen data. Additionally, to evaluate potential multicollinearity among covariates, the Variance Inflation Factor (VIF) was computed for all variables included in the Cox models. A VIF value greater than 10 was considered indicative of significant multicollinearity, while values below 5 were regarded as evidence of no substantial collinearity. Kaplan–Meier curves visualized complication incidence stratified by extreme organ aging status. Participants were categorized by baseline count of extremely aged organs (0, 1–3, > 3) for multivariable Cox regression assessing complication risk differentials, with corresponding Kaplan–Meier visualization. Additive interaction effects were evaluated through relative excess risk due to interaction (RERI) and attributable proportion (AP) metrics. To explore the specificity of organ aging-disease patterns in diabetes, stratified Cox proportional hazards regression analyses were conducted by baseline diabetes status (diabetes vs. no diabetes). The exposure was organ-specific age gap (per 1-unit increase), and outcomes included incident CKD, CVD, DR, all-cause death, and PAD. All models were adjusted for age, sex, ethnicity, Townsend deprivation index (TDI), current smoking status, use of antihypertensive and antidiabetic medications, systolic blood pressure (SBP), body mass index (BMI), total cholesterol, glucose levels, and other organ-specific age gaps. Multiplicative interaction terms (diabetes status × organ age gap) were incorporated into full Cox models to test interaction effects, with statistical significance determined by likelihood ratio tests (comparing models with/without interaction terms). All analyses utilized R statistical software version 4.2.2 (R Foundation for Statistical Computing).

Results

Cohort characteristics

Among 1979 enrolled diabetes patients, baseline comorbidities included CVD in 187 (9.45%), DR in 59 (2.98%), PAD in 35 (1.77%), and CKD in 34 (1.72%). Patients with any baseline complication (mean age: CVD: 62.00, DR: 61.24, PAD: 62.14, CKD: 62.41) were significantly older than those without complications (mean age: 59.43). The PAD group exhibited a higher proportion of current smokers (22.86%) compared to other groups (CVD: 10.70%, DR: 6.78%, CKD: 2.94%, no complication: 12.36%). Furthermore, patients with baseline DR had significantly higher systolic blood pressure (143.32mmHg) and HbA1c levels (7.91%) than diabetes patients in other categories (supplementary Table S4).

Organ age characteristics in patients with diabetes

Organ-specific age estimates for adipose tissue, artery, brain, heart, immune system, intestine, kidney, liver, lung, muscle, and pancreas were derived from the analysis of > 2000 plasma proteins. As shown in Fig. 1A, supplementary Fig. S1, and Table S5, the predictive performance of organ-specific aging models varied across organs and cohorts. In the original study's test cohort, brain (r = 0.710, MAE = 4.724 years) and artery (r = 0.710, MAE = 4.795 years) models

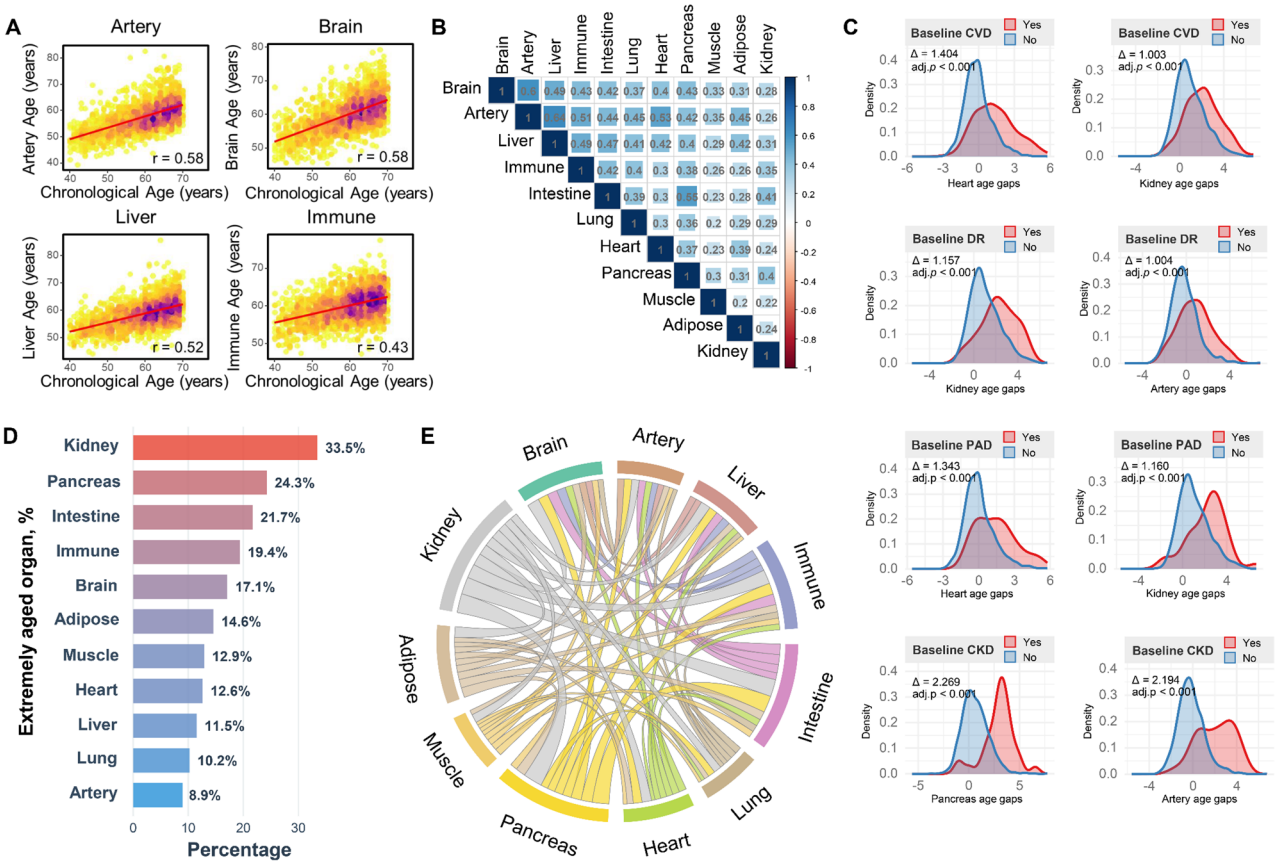

Fig. 1 Organ-specific aging patterns in diabetes. **A** Correlation between organ-specific biological ages and chronological age. Pearson correlation coefficients quantify association strength. **B** Pairwise correlations among 11 organ-specific biological ages. Heatmap intensity reflects Pearson correlation magnitudes. **C** Comparative distribution of organ age gaps in participants with versus without baseline diabetes complications. Differences assessed via age- and sex-adjusted linear regression. **D** Population prevalence ranking of extreme organ aging (organ age gap > 1.5 SD). **E** Co-aging network for extremely aged organs. Line thickness corresponds to participant counts with concurrent organ aging. CKD: chronic kidney disease; CVD: cardiovascular disease; DR: diabetic retinopathy; PAD: peripheral artery disease

exhibited the highest predictive accuracy, while kidney (r = 0.135, MAE = 6.960 years) and adipose (r = 0.248, MAE = 6.789 years) models had the lowest. In the current study's diabetes cohort, the top-performing models were also brain (r = 0.583, MAE = 4.784 years) and artery (r = 0.577, MAE = 5.329 years), whereas adipose (r = 0.178, MAE = 6.421 years) and muscle (r = 0.267, MAE = 6.217 years) models showed the lowest correlation with chronological age. Compared to the original study, the diabetes cohort had modestly reduced r values for most organs (e.g., immune: 0.539 vs. 0.429; intestine: 0.460 vs. 0.372) but similar or slightly lower MAEs (e.g., intestine: 6.106 vs. 5.511 years; pancreas: 6.576 vs. 5.693 years), indicating that the models maintain reasonable prediction error despite attenuated correlations in the diabetic population. Notably, 4 out of 11 organ models (lung, muscle, adipose, kidney) in the diabetes cohort had r < 0.3, accompanied by MAEs exceeding 6.1 years. Correlation analysis of organ age relationships revealed strong positive associations, most notably between liver and artery (r = 0.64), brain and artery (r = 0.60), pancreas and intestine (r = 0.55), heart and artery (r = 0.53), and immune system and artery (r = 0.51) (Fig. 1B).

Organ-specific age gaps were calculated as the residuals from linear regression models of predicted age against chronological age and subsequently z-scored within each aging model to normalize for differences in prediction accuracy. Analysis of organ-specific age gaps by complication status revealed distinct patterns of accelerated aging (Fig. 1C, supplementary Figure S2–S5). Cardiac and renal aging were significantly accelerated in patients with baseline CVD ($P < 0.001$). Compared to complication-free controls, renal and arterial aging were markedly pronounced in those with baseline DR (both $P < 0.001$). Cardiac and renal tissues exhibited the most severe aging acceleration in the PAD subgroup. In CKD patients, pancreatic (delta = 2.269, $P < 0.001$) and arterial aging (delta = 2.194, $P < 0.001$) demonstrated the strongest difference. Extreme organ aging was defined as an organ-specific age gap > 1.5 SD above the population

average. The prevalence of extreme aging was highest in kidney (33.5%), followed by pancreas (24.3%) and intestine (21.7%), and lower in artery (8.9%), lung (10.2%), and liver (11.5%) (Fig. 1D). Extremely aged kidney frequently co-occurred with extreme aging in pancreas, intestine, or immune system (Fig. 1E). Pairwise associations (measured by phi coefficient) were strongest between hepatic and arterial aging ($\phi = 0.33$), cardiac and arterial aging ($\phi = 0.33$), and pancreatic and intestinal aging ($\phi = 0.35$) (Supplementary Table S6).

Organ age estimates predict future diabetes complications

Among the 1,707 patients without baseline complications, during a median follow-up time of 12.71 years (IQR 12.71–14.34), 356 incident all-cause deaths (20.86%), 348 incident cardiovascular events (20.39%), 227 incident DR cases (13.30%), 88 incident PAD cases (5.16%), and 280 incident CKD cases (16.40%) occurred.

Following comprehensive adjustment for age, sex, ethnicity, TDI, current smoking status, use of antihypertensive and antidiabetic medications, SBP, BMI, total cholesterol, glucose levels, and other organ-specific age gaps, accelerated aging in specific organs demonstrated significant associations with incident complications in diabetes patients (Fig. 2A, supplementary Table S7). Accelerated cardiac aging (adjusted HR per 1-SD: 1.47, 95% CI: 1.32, 1.64; $P < 0.001$), brain aging (adjusted HR per 1. SD: 1.17, 95% CI: 1.04, 1.31; $P = 0.008$), and pancreatic aging (adjusted HR per 1-SD: 1.12, 95% CI: 1.00, 1.25; $P = 0.044$) were independently associated with increased risk of incident CVD. For incident DR, significant associations were observed with accelerated brain aging (adjusted HR per 1-SD: 1.25, 95% CI: 1.09, 1.44; $P = 0.001$) and muscular aging (adjusted HR per 1-SD: 1.15, 95% CI: 1.02, 1.31; $P = 0.028$). Accelerated brain aging also correlated with a higher risk of incident PAD (adjusted HR per 1-SD: 1.34, 95% CI: 1.07, 1.67; $P = 0.011$). Incident CKD risk was associated with accelerated arterial aging (adjusted HR per 1-SD: 1.21, 95% CI: 1.06, 1.38; $P = 0.005$) and pulmonary aging (adjusted HR per 1-SD: 1.19, 95% CI: 1.03, 1.36; $P = 0.014$). Furthermore, accelerated pulmonary aging was significantly associated with increased all-cause mortality risk in this diabetes population (adjusted HR per 1-SD: 1.19, 95% CI: 1.06, 1.34; $P = 0.002$). For overfitting, the Bootstrap-derived optimism values varied across the study endpoints, with the highest optimism value observed for PAD (0.0880), followed by DR (0.0535), CVD (0.0357), Mortality (0.0319), and CKD (0.0314). These values indicated that only PAD exhibited mild overfitting (optimism between 0.05 and 0.1) while no obvious overfitting was detected for the other endpoints (optimism < 0.05), suggesting good generalization ability of the models overall. For multicollinearity, the VIF analyses revealed that all covariates included in the models had VIF values well below 2, which ruled out the presence of significant multicollinearity in our models (Supplementary Table S8).

We further evaluated associations between extreme organ aging and complication risk in patients with diabetes (Fig. 2B–C, supplementary Table S9). After multivariable adjustment for demographic, clinical, biochemical parameters, and co-existing extreme organ aging, baseline extreme cardiac aging conferred the highest risk for incident CVD (adjusted HR: 2.92, 95% CI: 2.13, 3.99; $P < 0.001$), with significant associations also observed for extreme brain (adjusted HR: 1.43, 95% CI: 1.06, 1.92; $P = 0.019$), arterial (adjusted HR: 1.59, 95% CI: 1.06, 2.39; $P = 0.024$), and pancreatic aging (adjusted HR: 1.35, 95% CI: 1.04, 1.77; $P = 0.027$). Incident DR risk demonstrated significant associations with extreme aging in multiple organs: arterial (adjusted HR: 2.20, 95% CI: 1.36, 3.57; $P = 0.001$), brain (adjusted HR: 1.83, 95% CI: 1.29, 2.58; $P < 0.001$), muscular (adjusted HR: 1.67, 95% CI: 1.15, 2.42; $P = 0.007$), cardiac (adjusted HR: 1.66, 95% CI: 1.05, 2.63; $P = 0.030$), and pancreatic aging (adjusted HR: 1.47, 95% CI: 1.05, 2.05; $P = 0.024$). Extreme cardiac (adjusted HR: 2.49, 95% CI: 1.29, 4.80; $P = 0.007$) and arterial aging (adjusted HR: 2.34, 95% CI: 1.13, 4.85; $P = 0.022$) predicted incident PAD risk. For CKD risk, positive associations existed for all evaluated organs except brain, liver, and immune system tissues. Extreme cardiac (adjusted HR: 1.74, 95% CI: 1.24, 2.43; $P = 0.001$), brain (adjusted HR: 1.65, 95% CI: 1.25, 2.18; $P < 0.001$), pulmonary (adjusted HR: 95% CI: 1.62, 1.16, 2.27; $P = 0.005$), and pancreatic aging (adjusted HR: 1.34, 95% CI: 1.03, 1.75; $P = 0.029$) were significantly associated with all-cause mortality.

We introduced two elastic net regression models to further evaluate the stability across different proteomics-based organ aging assessment methods (supplementary Table S10). For CKD, key consistent findings included significant positive associations between CKD risk and both kidney and pancreas aging across all three models: kidney aging was linked to CKD via LASSO (adjusted HR per 1-SD: 1.18, 95% CI: 1.05, 1.31; $P = 0.004$), elastic net (adjusted HR per 1-SD: 1.57, 95% CI: 1.37, 1.80; $P < 0.001$), and mortality-based (adjusted HR per 1-SD: 1.68, 95% CI: 1.41,1.99; $P < 0.001$). Pancreas aging also showed consistent significance (LASSO: adjusted HR per 1-SD: 1.32, 95% CI: 1.17, 1.49; $P < 0.001$; elastic net: adjusted HR per 1-SD: 1.34, 95% CI: 1.14, 1.57; $P < 0.001$; mortality-based: adjusted HR per 1-SD: 1.32, 95% CI: 1.12, 1.56; $P = 0.001$). The mortality-based model further identified an additional significant link with adipose tissue aging (adjusted HR per 1-SD: 1.28, 95% CI: 1.11, 1.48; $P < 0.001$), which was non-significant in the LASSO model. For CVD, heart and pancreas aging showed consistent directional associations across all three methods.

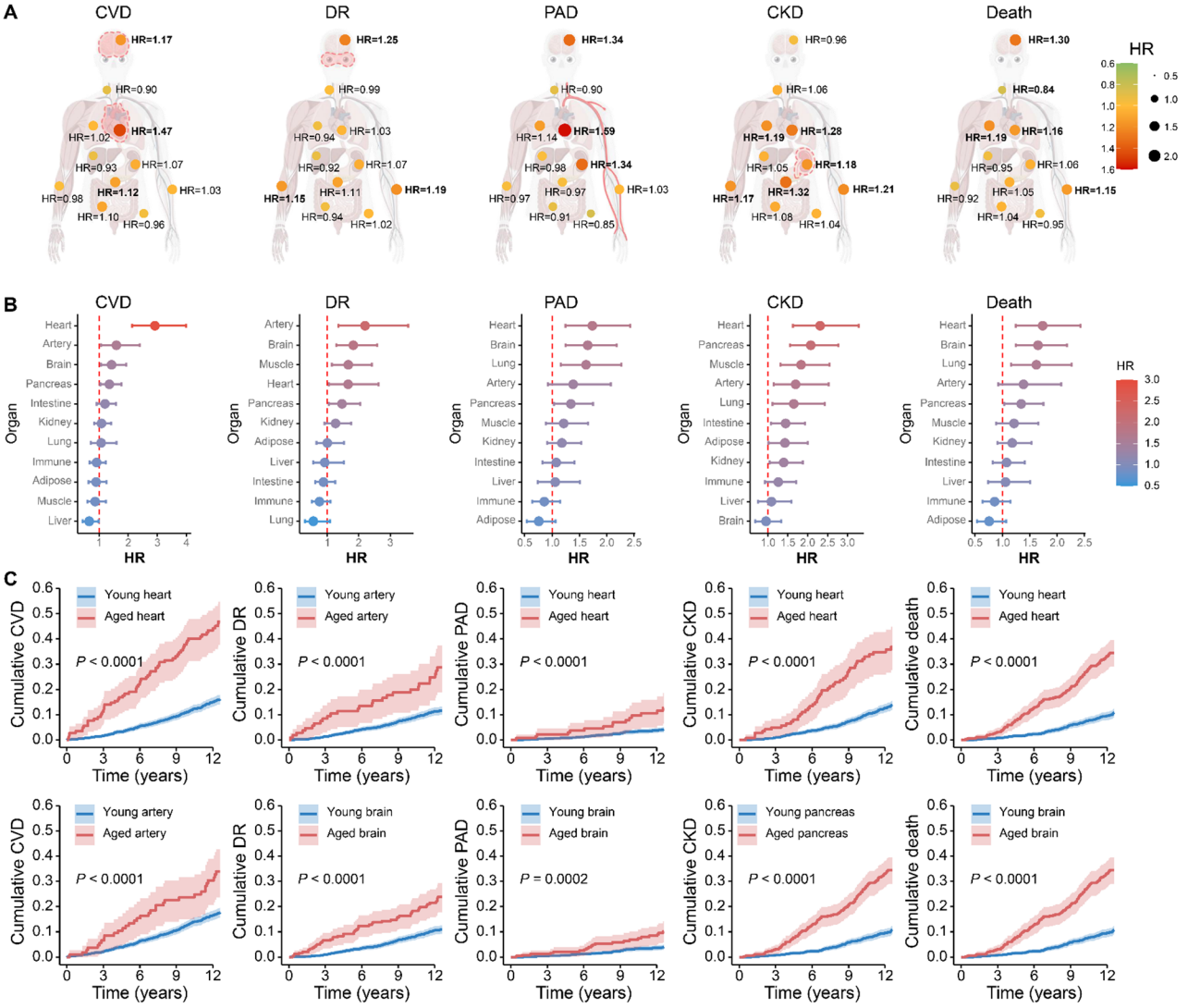

Fig. 2 Organ aging and complication risks in diabetes. **A** Associations between organ-specific age gaps and incident complications. Plot displays adjusted hazard ratios (HR) for cardiovascular disease (CVD), diabetic retinopathy (DR), peripheral artery disease (PAD), chronic kidney disease (CKD), and all-cause mortality. Dot size and color intensity scale with HR magnitude. Bolded markers indicate statistical significance ($P < 0.05$). Multivariable models adjusted for age, sex, ethnicity, Townsend deprivation index, smoking status, antihypertensive/antidiabetic medication use, systolic blood pressure, body mass index, total cholesterol, glucose levels, and concurrent organ aging gaps. **B** Relationships of extreme organ aging (> 1.5 SD above normative age) with complication risks. Forest plot visualizes adjusted HRs accounting for age, sex, ethnicity, Townsend deprivation index, smoking status, antihypertensive/antidiabetic medication use, systolic blood pressure, body mass index, total cholesterol, glucose levels, and coexisting extreme aging in other organs. **C** Cumulative incidence of diabetes complications stratified by baseline extreme organ aging status. Kaplan–Meier curves compare progression trajectories and log-rank *P*-values quantify between-group differences. CKD: chronic kidney disease; CVD: cardiovascular disease; DR: diabetic retinopathy; HR: hazard ratio; PAD: peripheral artery disease

The mortality-based model uncovered a novel significant link with artery aging (adjusted HR per 1-SD: 1.18, 95% CI: 1.00, 1.39; $P = 0.047$) not detected by the LASSO or elastic net models. For DR, brain aging was consistently linked to risk across all three models. The mortality-based model identified a new significant association with pancreas aging (adjusted HR per 1-SD: 1.40, 95% CI: 1.16, 1.70; $P < 0.001$) that was non-significant in the other two approaches. For all-cause mortality, brain and lung aging showed robust consistent associations across all three models.

Supplementary Table S11 presents adjusted HR and 95% CI for organ-specific age gap-outcome associations stratified by diabetes status, and interaction *P* values (adjusted for age, sex, ethnicity, TDI, current smoking status, use of antihypertensive and antidiabetic medications, SBP, BMI, total cholesterol, glucose levels, and other organ-specific age gaps). Significant interaction effects were observed for CKD (Adipose, Artery, Brain,

Immune, Intestine, Kidney, Liver, Lung, Pancreas; all $P<0.05$), CVD (Immune, Liver, Muscle; all $P<0.05$), DR (Artery, Heart, Immune, Intestine, Kidney, Pancreas; all $P<0.05$), and all-cause death (Brain, Immune, Muscle, Pancreas; all $P<0.05$). For example, Artery aging was significantly associated with DR risk in DM (adjusted HR per 1-SD: 1.19, 95% CI: 1.02, 1.39; $P=0.024$) but not in Non-DM (adjusted HR per 1-SD: 0.92, 95% CI: 0.71, 1.20; $P=0.538$); Immune aging was positively associated with death risk in Non-DM (adjusted HR per 1-SD: 1.06, 95% CI: 1.02, 1.11; $P=0.002$) but negatively in DM (adjusted HR per 1-SD: 0.84, 95% CI: 0.74, 0.95; $P=0.007$). Consistent positive associations across diabetes statuses were noted for Heart aging with CVD (DM: adjusted HR per 1-SD: 1.47; $P<0.001$; Non-DM: adjusted HR per 1-SD: 1.34; $P<0.001$) and Brain aging with DR (DM: adjusted HR per 1-SD: 1.25; $P=0.001$; Non-DM: adjusted HR per 1-SD: 1.23; $P=0.054$). For PAD, no significant interactions were found (all $P>0.05$), with consistent positive associations of Brain, Heart, and Kidney aging in both groups (all $P<0.05$).

Cumulative burden of multi-organ aging and complication risk

Organ aging frequently exhibited multi-system involvement, with complex interactions potentially existing between co-aged organs. Within our cohort, 502 individuals (25.4%) presented with extreme aging in a single organ at baseline, while 370 (18.7%) displayed two concurrently aged organs, and 537 (27.1%) exhibited extreme aging in three or more organ systems (Fig. 3A). Survival analysis demonstrated a graded increase in complication risk with escalating organ aging burden. Patients with baseline extreme aging in more than 3 organs faced significantly higher risks of incident CVD, DR, PAD, CKD, and all-cause mortality compared to those with no or only one to three extremely aged organs (Fig. 3B). After adjustment for age, sex, ethnicity, TDI, current smoking status, use of antihypertensive and antidiabetic

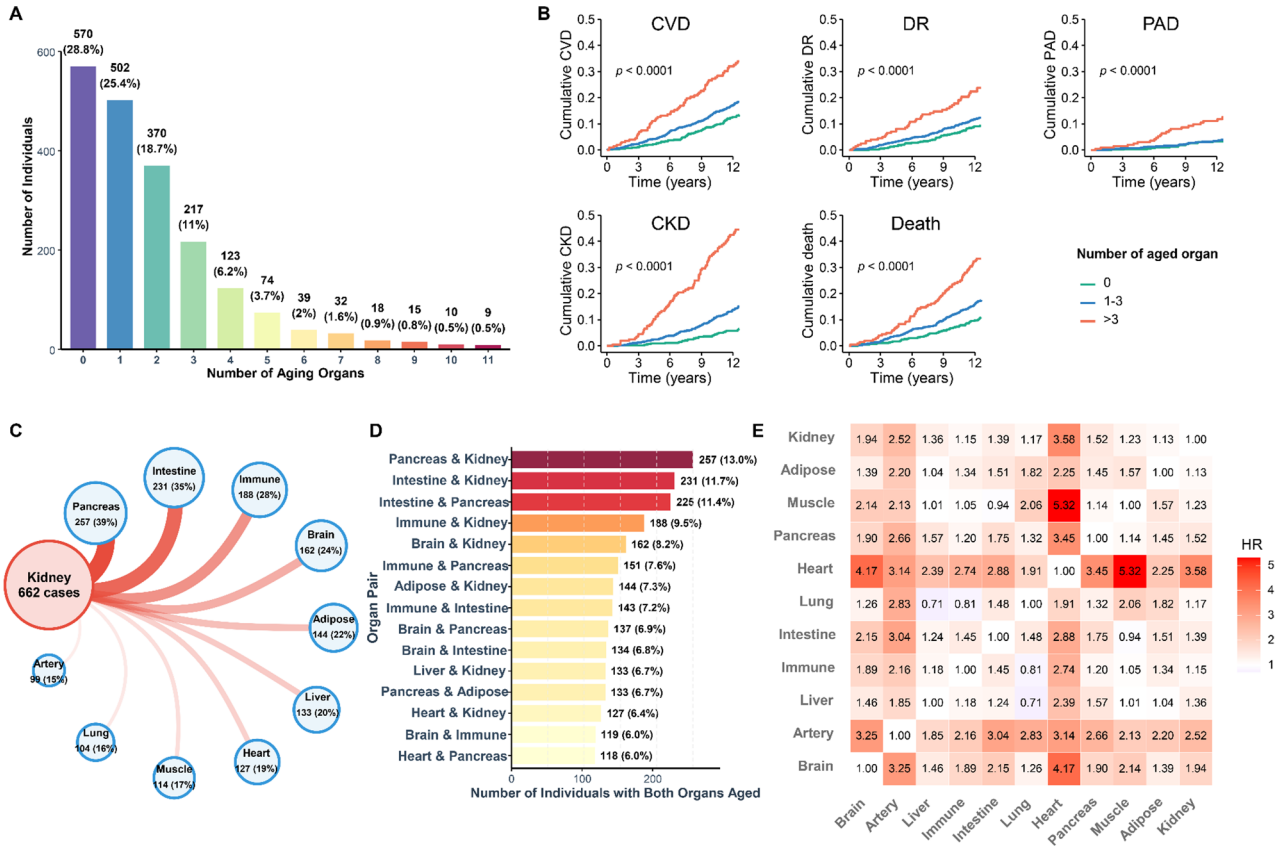

Fig. 3 Multiorgan aging and diabetes complication risks. **A** Population distribution of concurrent organ aging burden. Bar height indicates prevalence ranking of individuals with multiple extremely aged organs. **B** Dose–response relationship between number of extremely aged organs and incident complications. Kaplan–Meier curves compare cardiovascular disease (CVD), diabetic retinopathy (DR), peripheral artery disease (PAD), chronic kidney disease (CKD), and all-cause mortality risks (log-rank *P*-values shown). **C** Renal-centric co-aging network. Line thickness and circle size indicate frequency of concurrent extreme aging in connected organs. **D** Prevalence ranking of specific organ-pair co-aging combinations. **E** CVD risk associated with paired organ co-aging. Heatmap displays adjusted hazard ratios (color intensity) from multivariable Cox models accounting for age, sex, ethnicity, Townsend deprivation index, smoking status, antihypertensive/antidiabetic medication use, systolic blood pressure, body mass index, total cholesterol, and glucose levels

medications, SBP, BMI, total cholesterol, glucose levels, the CKD risk among patients with > 3 extremely aged organs was strikingly elevated, reaching 7.30-fold higher than diabetes patients without extreme organ aging at baseline (adjusted HR: 7.30, 95% CI: 4.77, 11.19; $P < 0.001$) (supplementary Table S12).

Analysis of multi-organ aging patterns revealed kidney aging as the most prevalent manifestation, frequently co-occurring with pancreatic (257 cases, 39.0% of kidney-aging individuals), intestinal (231 cases, 35.1%), and immune system aging (188 cases, 28.6%) (Fig. 3C). The most common organ-pair co-occurrences involved pancreas-kidney (257 cases, 13.0%), intestine-kidney (231 cases, 11.7%), and intestine-pancreas (225 cases, 11.4%) (Fig. 3D). Following adjustment for key covariates including demographics, TDI, smoking status, cardiometabolic medications (antihypertensive/antidiabetic), SBP, BMI, total cholesterol, and glucose levels, significant outcome associations emerged for specific organ-pair combinations: Concurrent heart and muscle aging strongly predicted CVD risk (adjusted HR: 5.32, 95% CI: 3.00, 9.41; $P < 0.001$) (Fig. 3E, supplementary Table S13). Similarly elevated CVD hazards were observed for heart-kidney (adjusted HR: 3.58, 95% CI: 2.39, 5.34; $P < 0.001$) and heart-brain aging pairs (adjusted HR: 4.17, 95% CI: 2.66, 6.52; $P < 0.001$). Co-aging of heart and lung demonstrated particularly robust associations with incident DR (adjusted HR: 8.80, 95% CI: 2.69, 28.77; $P < 0.001$) and PAD (adjusted HR: 11.25, 95% CI: 2.53, 49.99; $P < 0.001$) (supplementary Figure S6, Tables S14-S15). Lung-artery co-aging significantly correlated with CKD development (adjusted HR: 7.37, 95% CI: 3.42, 15.88; $P < 0.001$) and all-cause mortality (adjusted HR: 5.51, 95% CI: 3.07, 9.91; $P < 0.001$) (supplementary Tables S16–S17). Additive interaction analysis revealed synergistic effects of organ aging on CVD risk in diabetes (Table 1). While isolated heart aging increased CVD risk (adjusted HR: 2.89, 95% CI: 2.12, 3.95) and muscle aging showed no significant association (adjusted HR: 0.67, 95% CI: 0.43, 1.06), concurrent aging in both organs substantially elevated CVD risk (adjusted HR: 6.05, 95% CI: 3.41, 10.76). This interaction was statistically significant, with a relative excess risk due to interaction (RERI) of 3.49 (95% CI: 0.74, 8.16) and an attributable proportion (AP) of 0.58 (95% CI: 0.14, 0.74). Analyses for other complications are summarized in Supplementary Tables S18–S20. For all-cause mortality, significant additive interactions were observed between brain and artery aging (RERI: 2.23, 0.38, 4.73; AP: 0.52, 0.08, 0.71) and between artery and lung aging (RERI: 3.72, 0.93, 8.46; AP: 0.63, 0.20, 0.77) (Supplementary Table S21).

Discussion

This investigation enrolled 1979 individuals with diabetes, including 1707 without baseline complications, and provides the first comprehensive assessment of organ-specific aging patterns in this population, identifying accelerated organ aging as a significant predictor for multiple diabetes complications while evaluating the synergistic impact of and interactions between multi-organ aging processes on complication development. The convergence of results from the original LASSO model (Oh et al.), Goeminne et al.'s elastic net model (trained on physiological age), and mortality-based model (trained on survival outcomes) provides strong evidence that organ-specific aging is reliably associated with increased risk of diabetes complications. These three methods differ in their underlying objectives and statistical frameworks, yet they consistently validate key organ-complication links. This cross-method consistency directly confirms that our core conclusion is not dependent on a single analytical approach, underscoring its robustness. Moreover, the mortality-based model further enhances these findings by uncovering novel links. This superiority stems from its training on survival outcomes, which directly reflect the clinical impact of organ functional decline rather than chronological age (a temporal proxy) or the LASSO model's focus on variable selection. As highlighted by Goeminne et al., mortality-based aging models capture biological processes linked to disease progression and death more effectively, making them clinically actionable [18].

Previous study demonstrated the predictive value of organ-specific aging in the general population. Our works addressed the specificity of organ aging-disease patterns in diabetes, addressing the gap left by previous general population studies [17–19]. Diabetes modifies the associations between organ aging and most complications (CKD, CVD, DR, all-cause death), as evidenced by significant interaction effects for multiple organs. These diabetes-specific associations may reflect synergistic pathophysiological mechanisms: e.g., Artery aging synergizes with diabetes-induced vascular damage to enhance DR risk (significant in DM but not Non-DM); Pancreas aging (key to glucose metabolism) shows a stronger association with CKD in DM, likely due to dual impairments of pancreatic aging and diabetes on glucose homeostasis. Notably, immune aging exhibits contrasting associations with CVD/death risk across groups, which was positive in non-DM but negative (or non-significantly) in DM. This pattern may reflect dysregulated immune responses in diabetes that alter the pathogenic role of immune aging, a finding that requires further validation.

Multiple proteomic investigations have validated the utility of plasma proteomics for predicting diabetes and diabetes-related complications [20, 21]. For instance, Ye

Table 1 Interaction analysis between baseline organ aging and incident cardiovascular disease risk in diabetes

Organ pair		Adjusted HR (95%CI)				Additive joint interaction	
Organ1	Organ2	Both young	Organ1 aged	Organ2 aged	Both aged	RERI	AP
Brain	Artery	1.00 (Reference)	1.55 (1.13, 2.13)	2.16 (1.37, 3.39)	3.63 (2.16, 6.08)	0.92 (− 1.00, 3.43)	0.25 (− 0.47, 0.54)
Brain	Liver	1.00 (Reference)	1.80 (1.32, 2.46)	1.09 (0.71, 1.67)	1.57 (0.87, 2.83)	− 0.32 (− 1.42, 1.03)	− 0.21 (− 1.57, 0.22)
Brain	Immune	1.00 (Reference)	1.60 (1.13, 2.27)	0.97 (0.69, 1.35)	1.98 (1.29, 3.05)	0.41 (− 0.56, 1.53)	0.21 (− 0.44, 0.50)
Brain	Intestine	1.00 (Reference)	1.53 (1.05, 2.22)	1.29 (0.96, 1.74)	2.38 (1.60, 3.53)	0.56 (− 0.49, 1.75)	0.24 (− 0.31, 0.50)
Brain	Lung	1.00 (Reference)	1.83 (1.36, 2.46)	1.24 (0.81, 1.90)	1.42 (0.66, 3.03)	− 0.65 (− 1.83, 1.03)	− 0.46 (− 2.71, 0.02)
Brain	Heart	1.00 (Reference)	1.44 (1.02, 2.02)	3.04 (2.17, 4.26)	4.91 (3.12, 7.74)	1.44 (− 0.66, 4.28)	0.29 (− 0.23, 0.55)
Brain	Pancreas	1.00 (Reference)	1.78 (1.24, 2.55)	1.56 (1.18, 2.07)	2.29 (1.51, 3.49)	− 0.04 (− 1.17, 1.20)	− 0.02 (− 0.72, 0.32)
Brain	Muscle	1.00 (Reference)	1.58 (1.16, 2.16)	0.72 (0.46, 1.13)	2.23 (1.27, 3.93)	0.93 (− 0.21, 2.64)	0.42 (− 0.28, 0.63)
Brain	Adipose	1.00 (Reference)	1.88 (1.37, 2.58)	1.24 (0.86, 1.78)	1.56 (0.89, 2.71)	− 0.56 (− 1.62, 0.68)	− 0.36 (− 1.70, 0.12)
Brain	Kidney	1.00 (Reference)	1.55 (1.04, 2.30)	1.09 (0.82, 1.43)	2.07 (1.40, 3.06)	0.44 (− 0.53, 1.46)	0.21 (− 0.36, 0.50)
Artery	Liver	1.00 (Reference)	2.87 (1.87, 4.42)	0.98 (0.63, 1.51)	1.93 (1.09, 3.42)	− 0.92 (− 2.73, 0.85)	− 0.48 (− 2.15, 0.15)
Artery	Immune	1.00 (Reference)	2.61 (1.67, 4.08)	1.02 (0.75, 1.39)	2.28 (1.34, 3.88)	− 0.35 (− 2.08, 1.45)	− 0.15 (− 1.35, 0.33)
Artery	Intestine	1.00 (Reference)	2.06 (1.24, 3.39)	1.29 (0.98, 1.70)	3.33 (2.09, 5.32)	0.99 (− 0.80, 3.06)	0.30 (− 0.37, 0.58)
Artery	Lung	1.00 (Reference)	2.39 (1.63, 3.51)	1.08 (0.71, 1.64)	2.99 (1.32, 6.77)	0.52 (− 1.53, 4.35)	0.17 (− 1.25, 0.48)
Artery	Heart	1.00 (Reference)	2.29 (1.43, 3.67)	3.42 (2.47, 4.73)	3.79 (2.32, 6.21)	− 0.91 (− 3.23, 1.68)	− 0.24 (− 1.25, 0.23)
Artery	Pancreas	1.00 (Reference)	2.39 (1.46, 3.90)	1.47 (1.13, 1.93)	3.12 (1.93, 5.05)	0.26 (− 1.63, 2.31)	0.08 (− 0.75, 0.45)
Artery	Muscle	1.00 (Reference)	2.47 (1.67, 3.66)	0.82 (0.54, 1.22)	2.22 (1.09, 4.51)	− 0.07 (− 1.72, 2.32)	− 0.03 (− 1.54, 0.37)
Artery	Adipose	1.00 (Reference)	2.59 (1.69, 3.97)	1.12 (0.79, 1.60)	2.37 (1.32, 4.24)	− 0.34 (− 2.08, 1.68)	− 0.14 (− 1.41, 0.32)
Artery	Kidney	1.00 (Reference)	2.35 (1.40, 3.96)	1.10 (0.85, 1.44)	2.71 (1.70, 4.32)	0.26 (− 1.58, 2.02)	0.10 (− 0.79, 0.48)
Liver	Immune	1.00 (Reference)	1.08 (0.67, 1.77)	1.09 (0.79, 1.49)	1.21 (0.74, 1.97)	0.04 (− 0.86, 0.91)	0.03 (− 1.06, 0.44)
Liver	Intestine	1.00 (Reference)	1.13 (0.70, 1.83)	1.49 (1.13, 1.95)	1.36 (0.82, 2.25)	− 0.26 (− 1.23, 0.73)	− 0.19 (− 1.36, 0.25)
Liver	Lung	1.00 (Reference)	1.26 (0.86, 1.85)	1.33 (0.88, 2.00)	0.76 (0.31, 1.86)	− 0.83 (− 1.83, 0.40)	− 1.09 (− 5.63, − 0.45)
Liver	Heart	1.00 (Reference)	0.91 (0.57, 1.45)	3.53 (2.57, 4.85)	2.78 (1.66, 4.68)	− 0.67 (− 2.39, 1.36)	− 0.24 (− 1.32, 0.23)
Liver	Pancreas	1.00 (Reference)	0.85 (0.49, 1.47)	1.50 (1.15, 1.97)	1.75 (1.11, 2.75)	0.40 (− 0.54, 1.44)	0.23 (− 0.49, 0.52)
Liver	Muscle	1.00 (Reference)	1.13 (0.77, 1.66)	0.90 (0.61, 1.33)	1.01 (0.41, 2.46)	− 0.03 (− 0.92, 1.47)	− 0.03 (− 2.56, 0.44)
Liver	Adipose	1.00 (Reference)	1.20 (0.79, 1.83)	1.27 (0.89, 1.80)	1.12 (0.60, 2.09)	− 0.35 (− 1.30, 0.71)	− 0.31 (− 2.01, 0.17)
Liver	Kidney	1.00 (Reference)	0.91 (0.52, 1.60)	1.13 (0.87, 1.48)	1.43 (0.90, 2.25)	0.39 (− 0.49, 1.25)	0.27 (− 0.51, 0.59)
Immune	Intestine	1.00 (Reference)	1.03 (0.73, 1.47)	1.41 (1.05, 1.89)	1.56 (1.04, 2.36)	0.12 (− 0.66, 0.96)	0.08 (− 0.61, 0.40)
Immune	Lung	1.00 (Reference)	1.21 (0.90, 1.62)	1.46 (0.93, 2.29)	0.86 (0.45, 1.65)	− 0.80 (− 1.82, 0.16)	− 0.93 (− 3.54, − 0.22)
Immune	Heart	1.00 (Reference)	1.04 (0.76, 1.44)	3.45 (2.49, 4.77)	3.18 (1.92, 5.27)	− 0.31 (− 2.07, 1.87)	− 0.10 (− 1.01, 0.31)
Immune	Pancreas	1.00 (Reference)	1.19 (0.83, 1.70)	1.70 (1.28, 2.25)	1.43 (0.95, 2.14)	− 0.46 (− 1.30, 0.34)	− 0.32 (− 1.20, 0.11)
Immune	Muscle	1.00 (Reference)	1.10 (0.82, 1.49)	0.88 (0.57, 1.34)	1.06 (0.56, 2.01)	0.08 (− 0.68, 1.08)	0.08 (− 1.33, 0.43)
Immune	Adipose	1.00 (Reference)	1.05 (0.76, 1.45)	1.14 (0.78, 1.67)	1.39 (0.85, 2.27)	0.19 (− 0.60, 1.11)	0.14 (− 0.71, 0.46)
Immune	Kidney	1.00 (Reference)	1.13 (0.78, 1.65)	1.19 (0.91, 1.57)	1.26 (0.84, 1.88)	− 0.07 (− 0.77, 0.60)	− 0.05 (− 0.81, 0.32)
Intestine	Lung	1.00 (Reference)	1.42 (1.08, 1.86)	1.02 (0.60, 1.73)	1.60 (0.95, 2.70)	0.16 (− 0.87, 1.32)	0.10 (− 0.89, 0.44)
Intestine	Heart	1.00 (Reference)	1.46 (1.10, 1.94)	3.67 (2.63, 5.13)	3.61 (2.24, 5.83)	− 0.52 (− 2.45, 1.79)	− 0.14 (− 1.00, 0.28)
Intestine	Pancreas	1.00 (Reference)	1.23 (0.85, 1.76)	1.39 (1.01, 1.92)	1.94 (1.40, 2.68)	0.32 (− 0.51, 1.10)	0.16 (− 0.33, 0.45)
Intestine	Muscle	1.00 (Reference)	1.54 (1.17, 2.01)	0.99 (0.63, 1.53)	1.04 (0.58, 1.87)	− 0.48 (− 1.33, 0.45)	− 0.46 (− 2.16, 0.04)
Intestine	Adipose	1.00 (Reference)	1.41 (1.06, 1.88)	1.11 (0.74, 1.67)	1.65 (1.05, 2.58)	0.13 (− 0.74, 1.09)	0.08 (− 0.68, 0.40)
Intestine	Kidney	1.00 (Reference)	1.51 (1.06, 2.15)	1.16 (0.86, 1.55)	1.54 (1.09, 2.18)	− 0.13 (− 0.93, 0.58)	− 0.08 (− 0.72, 0.28)
Lung	Heart	1.00 (Reference)	1.29 (0.87, 1.93)	3.52 (2.63, 4.72)	2.28 (0.71, 7.29)	− 1.54 (− 3.58, 3.52)	− 0.67 (− 5.15, − 0.13)
Lung	Pancreas	1.00 (Reference)	1.12 (0.66, 1.91)	1.59 (1.22, 2.08)	1.51 (0.90, 2.54)	− 0.20 (− 1.27, 0.92)	− 0.13 (− 1.29, 0.29)
Lung	Muscle	1.00 (Reference)	1.00 (0.65, 1.53)	0.79 (0.53, 1.18)	2.01 (0.94, 4.28)	1.21 (− 0.01, 3.50)	0.61 (− 0.27, 0.83)
Lung	Adipose	1.00 (Reference)	0.93 (0.57, 1.51)	1.09 (0.77, 1.55)	1.85 (1.03, 3.33)	0.83 (− 0.21, 2.32)	0.45 (− 0.32, 0.69)
Lung	Kidney	1.00 (Reference)	1.19 (0.71, 2.01)	1.19 (0.92, 1.54)	1.28 (0.74, 2.21)	− 0.10 (− 1.10, 0.90)	− 0.08 (− 1.33, 0.34)
Heart	Pancreas	1.00 (Reference)	3.37 (2.35, 4.84)	1.47 (1.11, 1.95)	4.33 (2.85, 6.59)	0.49 (− 1.46, 2.79)	0.11 (− 0.48, 0.42)
Heart	Muscle	1.00 (Reference)	2.89 (2.12, 3.95)	0.67 (0.43, 1.06)	6.05 (3.41, 10.76)	3.49 (0.74, 8.16)	0.58 (0.14, 0.74)
Heart	Adipose	1.00 (Reference)	3.76 (2.73, 5.18)	1.16 (0.80, 1.68)	2.68 (1.57, 4.55)	− 1.25 (− 3.01, 0.78)	− 0.47 (− 1.72, 0.09)
Heart	Kidney	1.00 (Reference)	3.15 (2.17, 4.57)	1.15 (0.87, 1.52)	4.18 (2.73, 6.40)	0.88 (− 0.97, 3.10)	0.21 (− 0.34, 0.50)
Pancreas	Muscle	1.00 (Reference)	1.59 (1.22, 2.07)	0.90 (0.57, 1.43)	1.32 (0.76, 2.30)	− 0.17 (− 1.04, 0.86)	− 0.13 (− 1.33, 0.26)
Pancreas	Adipose	1.00 (Reference)	1.56 (1.18, 2.06)	1.13 (0.73, 1.74)	1.67 (1.09, 2.57)	− 0.01 (− 0.91, 0.91)	− 0.01 (− 0.76, 0.34)
Pancreas	Kidney	1.00 (Reference)	1.55 (1.10, 2.18)	1.11 (0.82, 1.51)	1.70 (1.21, 2.39)	0.05 (− 0.74, 0.75)	0.03 (− 0.51, 0.35)

Table 1 (continued)

Organ pair		Adjusted HR (95%CI)				Additive joint interaction	
Organ1	Organ2	Both young	Organ1 aged	Organ2 aged	Both aged	RERI	AP
Muscle	Adipose	1.00 (Reference)	0.73 (0.46, 1.14)	1.09 (0.76, 1.56)	1.57 (0.88, 2.79)	0.75 (−0.12, 1.98)	0.48 (−0.28, 0.73)
Muscle	Kidney	1.00 (Reference)	0.71 (0.42, 1.22)	1.13 (0.87, 1.46)	1.28 (0.79, 2.09)	0.44 (−0.29, 1.26)	0.34 (−0.42, 0.64)
Adipose	Kidney	1.00 (Reference)	1.33 (0.86, 2.05)	1.22 (0.93, 1.59)	1.28 (0.82, 1.98)	−0.27 (−1.14, 0.51)	−0.21 (−1.18, 0.23)

Hazard ratios were adjusted for age, sex, ethnicity, Townsend deprivation index, current smoking status, use of antihypertensive or antidiabetic medications, systolic blood pressure, body mass index, total cholesterol, and glucose levels. AP: attributable proportion; CI: confidence interval; HR: hazard ratio; RERI: relative excess risk due to interaction

et al. developed an 11-plasma-protein model via LASSO regression in 2094 individuals with diabetes that predicted CKD development (HR 1.78 per SD increase; 95% CI: 1.44, 2.20) [22]. Similarly, Yu and colleagues analyzed plasma proteomics from 1859 UK Biobank participants with diabetes, demonstrating that LASSO-selected 45-protein panels significantly improved PAD risk stratification [23]. Extending beyond individual biomarkers, our study quantifies organ-specific biological aging through plasma proteomics, identifying four organs whose accelerated aging demonstrates complication-specific associations: CVD risk was predominantly linked to cardiac aging (HR 2.92), while DR correlated most strongly with vascular and cerebral aging (HR 2.20 and 1.83, respectively). This organ-centric approach enables multi-complication risk assessment from a single proteomic assay. Collectively, these findings demonstrate that plasma proteomics not only refines complication prediction but also advances precision medicine by facilitating early intervention through simultaneous evaluation of organ-specific vulnerability in diabetes.

Type 2 diabetes manifests as an age-related disorder wherein insulin resistance accelerates β-cell senescence, driving functional decline and metabolic deterioration [24–26]. Beyond pancreatic cell, adipose tissue senescence independently correlates with diabetes pathogenesis [27]. Systemic organ aging is further evidenced in diabetes complications. Renal biopsies from diabetic nephropathy patients demonstrate elevated senescence markers (SA-β-gal and p16INK4A) in tubules and podocytes, while cardiac stem cell aging promoted by diabetes-induced ROS contributes to heart failure [28–30]. Critically, diabetes-organ aging relationships involve self-reinforcing cycles. Senescent cells propagate secondary senescence in adjacent and remote tissues through the senescence-associated secretory phenotype, creating a pathological cascade [25]. Research on diabetes-associated senescence holds significant translational potential, as evidenced by senolytic interventions [31]. Studies using transgenic INK-ATTAC models or oral ABT263 demonstrate that selective clearance of senescent cells (senolysis) enhances glucose homeostasis and β-cell function while attenuating aging markers and senescence-associated secretory phenotypes [8]. Complementing this approach, cell-based regenerative therapies exhibit potent anti-inflammatory and reparative effects in diabetic kidney disease (DKD). Preclinical evidence from experimental models and systematic analyses demonstrates that mesenchymal stromal cells (MSCs) and cell-derived products improve renal function and attenuate diabetic kidney injury, as evidenced by reduced proteinuria, improved glomerular histopathology (including mesangial matrix expansion and basement membrane thickening), decreased interstitial fibrosis, and reduced oxidative stress biomarkers in DKD models, with observed modulation of autophagy pathways and pro-fibrotic cytokine profiles [32, 33]. In the lowest-dose cohort of the randomized, placebo-controlled NEPHSTROM phase 1b/2a trial (N = 16 adults with type 2 diabetes and progressive DKD), a single intravenous infusion of 80×10^6 CD362-selected allogeneic MSCs (ORBCEL-M) demonstrated a significantly lower median annual rate of eGFR decline compared to placebo over 18 months (as measured by CKD-EPI and MDRD equations), despite no significant difference in measured GFR (mGFR) [34]. Beyond tissue regeneration, emerging evidence indicates MSCs and their extracellular vesicles exert senotherapeutic effects, notably reducing senescence-associated β-galactosidase expression in glomerular and interstitial compartments [35]. This work provides the first comprehensive characterization of multi-organ aging in diabetes and its association with complication risks, extending beyond the conventional focus on pancreatic islet senescence to establish broader implications for both aging biology and diabetes management. Our findings redefine pathological aging paradigms in diabetes, offering clinically relevant insights for developing targeted anti-aging therapeutics to mitigate long-term complications.

Strengths and limitations

This study used three validated proteomics-based methodologies to quantify multi-organ aging in diabetes, establishing significant associations between accelerated organ aging and complication risks while evaluating cumulative and interactive effects across organ systems. These findings advance both risk stratification paradigms and fundamental research on biological aging in diabetes. Important limitations warrant acknowledgment: First, complication diagnoses, though clinically

validated through hospital records, may be influenced by undetected baseline conditions. Second, the generalizability of our findings across diverse racial/ethnic groups remains to be fully verified. The organ-specific aging algorithm was developed in the UK Biobank and externally validated in independent US-based cohorts, but further verification in more diverse populations is needed to confirm its broader applicability. Moreover, biological heterogeneity across different racial/ethnic groups may require additional model calibration, which underscores the need for future studies in diverse cohorts. Third, the organ specificity definition used herein (≥ fourfold expression in GTEx) is relatively crude and may not fully reflect functional organ aging. While this definition is widely used in high-impact studies, its limitations are acknowledged, as no superior alternatives exist currently. Additionally, Uhlen et al. adopted a fivefold threshold for tissue-specific proteins, indicating inconsistent cut-offs in existing literature [36]. Moreover, the term "tissue-specific" is debated due to arbitrary cut-offs, as many proteins labeled as such are actually expressed in multiple tissues. Future studies should explore more accurate, technology-driven definitions to enhance understanding of organ-specific aging and diabetic complications. Forth, a potential limitation of this study is the variable predictive accuracy of the organ-specific aging models. 4 models in the current cohort had $r < 0.3$, a threshold often used to exclude models with insufficient predictive power in previous studies. Although we retained these models to explore their potential associations with diabetes complications, the low r values and high MAEs suggest that their predicted ages may not reliably reflect true organ aging processes. Therefore, interpretations of results related to these low-accuracy models should be made with caution. Future studies could optimize these models by incorporating additional organ-specific proteins or adjusting for diabetes-related confounders (e.g., HbA1c, medication use) to improve predictive performance. Fifth, accumulating evidence has demonstrated that lifestyle modifications and certain pharmacological exposures (e.g., ibuprofen, glucosamine) can modulate organ-specific aging. However, as a retrospective cohort study, the UK Biobank lacks longitudinal measurements of organ age before and after such interventions. This constraint prevents us from evaluating how interventions regulate organ aging dynamics and inferring causal relationships between interventions, organ aging changes, and diabetes complication risk, which is key evidence for the translational utility of organ aging clocks. Therefore, future studies are needed to address this gap, particularly well-designed prospective studies that dynamically track organ age changes alongside targeted interventions to clarify their potential clinical applications.

Conclusions

This plasma proteomics study establishes accelerated multiorgan aging as a significant risk determinant for macrovascular and microvascular complications in diabetes, demonstrating a dose-dependent relationship between cumulative organ aging burden and clinical outcomes. These findings advance geroscience-oriented diabetes care by enabling improved long-term risk stratification, early pathological aging detection, and targeted multiorgan monitoring protocols.

Supplementary Information

The online version contains supplementary material available at https://doi.org/10.1186/s12933-026-03111-5.

Supplementary Material 1

Supplementary Material 2

Acknowledgements

We express profound gratitude to Hamilton Se-Hwee Oh at Stanford University for his sophisticated guidance in developing statistical approaches for organ biological age estimation using plasma proteomic data, which enhanced methodological rigor throughout this investigation. This research has been conducted using the UK Biobank Resource under Application Number #97155.

Author contributions

K.F.D, and S.Y. designed and conducted the research. S.Y., Z.Y.L., and Y.J.S wrote the manuscript. S.Y., Z.Y.Z, and Y.J.S. performed the data management and statistical analyses. S.Y., Z.Y.L., Y.J.S., K.T.S., J.J.G., Z.Y.Z and K.F.D. read and approved the final manuscript. K.F.D. and Z.Y.Z are the guarantor of this work and, as such, have full access to all the data in the study and takes responsibility for the integrity of the data and the accuracy of the data analysis.

Funding

The research reported in this publication was supported by the Noncommunicable Chronic Diseases-National Science and Technology Major Project (grant number 2025ZD0548200) and the Postdoctoral Fellowship Program (Grade C) of China Postdoctoral Science Foundation under Grant Number GZC20251535. The study funder was not involved in the design of the study; the collection, analysis, and interpretation of data; writing the report; and did not impose any restrictions regarding the publication of the report.

Data availability

The dataset is available in the UK Biobank website (https://www.ukbiobank.ac.uk/).

Declarations

Ethics approval and consent to participate

The UK Biobank study was approved by the North West Multi-centre Research Ethics Committee (REC reference numbers 11/NW/0382, 16/NW/0274, and 21/NW/0157). All participants provided written informed consent.

Consent for publication

All authors agreed and approved the publication of the current manuscript.

Competing interests

The authors declare no competing interests.

Author details

[1]State Key Laboratory of Cardiovascular Disease, Beijing, China

[2]Cardiometabolic Medicine Center, National Clinical Research Center for Cardiovascular Diseases, State Key Laboratory of Cardiovascular Disease, Fuwai Hospital, National Center for Cardiovascular Diseases, Chinese Academy of Medical Sciences and Peking Union Medical College, A 167 Beilishi Rd, Xicheng District, Beijing 100037, China
[3]Department of MedicineMetropolitan Hospital Center, New York Medical College, New York, NY, USA
[4]Department of Pathology, The Affiliated Hospital of Qingdao University, Qingdao, China
[5]Department of Cardiology, Fuwai Hospital, National Center for Cardiovascular Diseases, Chinese Academy of Medical Sciences and Peking Union Medical College, A 167 Beilishi Rd, Xicheng District, Beijing 100037, China
[6]National Clinical Research Center for Cardiovascular Diseases, Beijing, China

Received: 29 October 2025 / Accepted: 3 February 2026
Published online: 15 February 2026

References

1. Sun H, Saeedi P, Karuranga S, Pinkepank M, Ogurtsova K, Duncan BB, et al. IDF diabetes atlas: global, regional and country-level diabetes prevalence estimates for 2021 and projections for 2045. Diabetes Res Clin Pract. 2022;183:109119.
2. American Diabetes Association Professional Practice Committee. 12. Retinopathy, Neuropathy, and Foot Care: Standards of Care in Diabetes-2024. Diabetes Care. 2024;47(Suppl 1):S231–43.
3. Nakagawa T, Tanabe K, Croker BP, Johnson RJ, Grant MB, Kosugi T, et al. Endothelial dysfunction as a potential contributor in diabetic nephropathy. Nat Rev Nephrol. 2011;7(1):36–44.
4. Seferović PM, Petrie MC, Filippatos GS, Anker SD, Rosano G, Bauersachs J, et al. Type 2 diabetes mellitus and heart failure: a position statement from the Heart Failure Association of the European Society of Cardiology. Eur J Heart Fail. 2018;20(5):853–72.
5. American Diabetes Association Professional Practice Committee. 10. Cardiovascular Disease and Risk Management: Standards of Care in Diabetes-2024. Diabetes Care. 2024 Jan 1;47(Suppl 1):S179–218.
6. Huang ES, Laiteerapong N, Liu JY, John PM, Moffet HH, Karter AJ. Rates of complications and mortality in older patients with diabetes mellitus: the diabetes and aging study. JAMA Intern Med. 2014;174(2):251–8.
7. Kalyani RR, Golden SH, Cefalu WT. Diabetes and aging: unique considerations and goals of care. Diabetes Care. 2017;40(4):440–3.
8. Aguayo-Mazzucato C, Andle J, Lee TB, Midha A, Talemal L, Chipashvili V, et al. Acceleration of β cell aging determines diabetes and senolysis improves disease outcomes. Cell Metab. 2019;30(1):129-142.e4.
9. Helman A, Klochendler A, Azazmeh N, Gabai Y, Horwitz E, Anzi S, et al. p16(Ink4a)-induced senescence of pancreatic beta cells enhances insulin secretion. Nat Med. 2016;22(4):412–20.
10. Horvath S, Raj K. DNA methylation-based biomarkers and the epigenetic clock theory of ageing. Nat Rev Genet. 2018;19(6):371–84.
11. Gao C, Amador C, Walker RM, Campbell A, Madden RA, Adams MJ, et al. Phenome-wide analyses identify an association between the parent-of-origin effects dependent methylome and the rate of aging in humans. Genome Biol. 2023;24(1):117.
12. Bahour N, Cortez B, Pan H, Shah H, Doria A, Aguayo-Mazzucato C. Diabetes mellitus correlates with increased biological age as indicated by clinical biomarkers. Geroscience. 2022;44(1):415–27.
13. Williams SA, Kivimaki M, Langenberg C, Hingorani AD, Casas JP, Bouchard C, et al. Plasma protein patterns as comprehensive indicators of health. Nat Med. 2019;25(12):1851–7.
14. Chen ZZ, Gerszten RE. Metabolomics and proteomics in type 2 diabetes. Circ Res. 2020;126(11):1613–27.
15. Oh HSH, Le Guen Y, Rappoport N, Urey DY, Farinas A, Rutledge J, et al. Plasma proteomics links brain and immune system aging with healthspan and longevity. Nat Med. 2025;31(8):2703–11.
16. Sun BB, Chiou J, Traylor M, Benner C, Hsu YH, Richardson TG, et al. Plasma proteomic associations with genetics and health in the UK Biobank. Nature. 2023;622(7982):329–38.
17. Oh HSH, Rutledge J, Nachun D, Pálovics R, Abiose O, Moran-Losada P, et al. Organ aging signatures in the plasma proteome track health and disease. Nature. 2023;624(7990):164–72.
18. Goeminne LJ, Vladimirova A, Eames A, Tyshkovskiy A, Argentieri MA, Ying K, et al. Plasma protein-based organ-specific aging and mortality models unveil diseases as accelerated aging of organismal systems. Cell metabolism [Internet]. 2025 Jan 7 [cited 2025 Dec 21];37(1). Available from: https://pubmed.ncbi.nlm.nih.gov/39488213/.
19. Tian YE, Cropley V, Maier AB, Lautenschlager NT, Breakspear M, Zalesky A. Heterogeneous aging across multiple organ systems and prediction of chronic disease and mortality. Nat Med. 2023;29(5):1221–31.
20. Li R, Tian S, Liu J, Li R, Zhu K, Lu Q, et al. Modifiable risk factors and plasma proteomics in relation to complications of type 2 diabetes. Nat Commun. 2025;16(1):2896.
21. Xie R, Vlaski T, Trares K, Herder C, Holleczek B, Brenner H, et al. Large-scale proteomics improve risk prediction for type 2 diabetes. Diabetes Care. 2025;48(6):922–6.
22. Ye Z, Zhang Y, Zhang Y, Yang S, He P, Liu M, et al. Large-scale proteomics improve prediction of chronic kidney disease in people with diabetes. Diabetes Care. 2024;47(10):1757–63.
23. Yu H, Zhang J, Qian F, Yao P, Xu K, Wu P, et al. Large-scale plasma proteomics improves prediction of peripheral artery disease in individuals with type 2 diabetes: a prospective cohort study. Diabetes Care. 2025;48:dc241696.
24. Grootaert MOJ. Cell senescence in cardiometabolic diseases. NPJ Aging. 2024;10(1):46.
25. Palmer AK, Tchkonia T, LeBrasseur NK, Chini EN, Xu M, Kirkland JL. Cellular senescence in type 2 diabetes: a therapeutic opportunity. Diabetes. 2015;64(7):2289–98.
26. Palmer AK, Gustafson B, Kirkland JL, Smith U. Cellular senescence: at the nexus between ageing and diabetes. Diabetologia. 2019;62(10):1835–41.
27. Liu Z, Wu KKL, Jiang X, Xu A, Cheng KKY. The role of adipose tissue senescence in obesity- and ageing-related metabolic disorders. Clin Sci (Lond). 2020;134(2):315–30.
28. Rota M, LeCapitaine N, Hosoda T, Boni A, De Angelis A, Padin-Iruegas ME, et al. Diabetes promotes cardiac stem cell aging and heart failure, which are prevented by deletion of the p66shc gene. Circ Res. 2006;99(1):42–52.
29. Fomison-Nurse I, Saw EEL, Gandhi S, Munasinghe PE, Van Hout I, Williams MJA, et al. Diabetes induces the activation of pro-ageing miR-34a in the heart, but has differential effects on cardiomyocytes and cardiac progenitor cells. Cell Death Differ. 2018;25(7):1336–49.
30. Verzola D, Gandolfo MT, Gaetani G, Ferraris A, Mangerini R, Ferrario F, et al. Accelerated senescence in the kidneys of patients with type 2 diabetic nephropathy. Am J Physiol Renal Physiol. 2008;295(5):F1563-1573.
31. Chaib S, Palmer AK, Wyles SP, Musi N, Kirkland JL, Tchkonia T. Translating cellular senescence research into clinical practice for metabolic disease. Nat Rev Endocrinol. 2025;22:102.
32. Hickson LJ, Abedalqader T, Ben-Bernard G, Mondy JM, Bian X, Conley SM, et al. A systematic review and meta-analysis of cell-based interventions in experimental diabetic kidney disease. Stem Cells Transl Med. 2021;10(9):1304–19.
33. He J, Liu B, Du X, Wei Y, Kong D, Feng B, et al. Amelioration of diabetic nephropathy in mice by a single intravenous injection of human mesenchymal stromal cells at early and later disease stages is associated with restoration of autophagy. Stem Cell Res Ther. 2024;15(1):66.
34. Perico N, Remuzzi G, Griffin MD, Cockwell P, Maxwell AP, Casiraghi F, et al. Safety and preliminary efficacy of mesenchymal stromal cell (ORBCEL-M) therapy in diabetic kidney disease: a randomized clinical trial (NEPHSTROM). J Am Soc Nephrol. 2023;34(10):1733–51.
35. Patel HA, Wang J, Zinn CJ, Learmonth M, Lerman LO, Wolfram J, et al. Fortifying the diabetic kidney disease treatment armamentarium: multitarget senotherapeutic and regenerative strategies. J Am Soc Nephrol. 2025;36(8):1655–8.
36. Uhlén M, Fagerberg L, Hallström BM, Lindskog C, Oksvold P, Mardinoglu A, et al. Proteomics. Tissue-based map of the human proteome. Science. 2015;347(6220):1260419.

Publisher's Note